Title

An extreme-preserving long-term gridded daily precipitation data set for the conterminous United States

Journal

Journal of Hydrometeorology, 22(7)

ISSN

1525-755X

Authors

Pierce, David W

Su, Lu

Cayan, Daniel R

et al.

Publication Date

2021-05-05

DOI

10.1175/jhm-d-20-0212.1

Peer reviewed

An Extreme-Preserving Long-Term Gridded Daily Precipitation Dataset for the Conterminous United States

DAVID W. PIERCE,[a] LU SU,[b] DANIEL R. CAYAN,[a] MARK D. RISSER,[c] BEN LIVNEH,[d] AND DENNIS P. LETTENMAIER[b]

[a] *Climate, Atmospheric Sciences, and Physical Oceanography, Scripps Institution of Oceanography, La Jolla, California*
[b] *Department of Geography, University of California, Los Angeles, Los Angeles, California*
[c] *Lawrence Berkeley National Laboratory, Berkeley, California*
[d] *CIRES, University of Colorado Boulder, Boulder, Colorado*

(Manuscript received 2 September 2020, in final form 8 March 2021)

ABSTRACT: Extreme daily precipitation contributes to flooding that can cause significant economic damages, and so is important to properly capture in gridded meteorological datasets. This work examines precipitation extremes, the mean precipitation on wet days, and fraction of wet days in two widely used gridded datasets over the conterminous United States. Compared to the underlying station observations, the gridded data show a 27% reduction in annual 1-day maximum precipitation, 25% increase in wet day fraction, 1.5–2.5 day increase in mean wet spell length, 30% low bias in 20-yr return values of daily precipitation, and 25% decrease in mean precipitation on wet days. It is shown these changes arise primarily from the time adjustment applied to put the precipitation gauge observations into a uniform time frame, with the gridding process playing a lesser role. A new daily precipitation dataset is developed that omits the time adjustment (as well as extending the gridded data by 7 years) and is shown to perform significantly better in reproducing extreme precipitation metrics. When the new dataset is used to force a land surface model, annually averaged 1-day maximum runoff increases 38% compared to the original data, annual mean runoff increases 17%, evapotranspiration drops 2.3%, and fewer wet days leads to a 3.3% increase in estimated solar insolation. These changes are large enough to affect portrayals of flood risk and water balance components important for ecological and climate change applications across the CONUS.

KEYWORDS: Extreme events; Precipitation; Runoff; Hydrology; Data processing; Surface observations

1. Introduction

Extreme weather events take a heavy toll on the U.S. economy, with the largest events totaling almost $1.8 trillion in damages (inflation adjusted) from 1980 to early 2020, and weather-related flooding alone responsible for 33 disasters costing $1 billion or more during that period (Smith 2020). Understanding historical extremes is also important for assessing climate change (Donat et al. 2016) and its ecological impacts (Knapp et al. 2008). It is important to ensure that meteorological datasets accurately represent extreme precipitation statistics given the significant economic and ecological impacts of heavy precipitation.

Extreme precipitation statistics can be calculated from long-term precipitation gauge records, although such instruments have foibles (e.g., Groisman and Legates 1994). Some gridded precipitation products blend gauge observations with other data, such as satellite estimates of precipitation, as in the CPU Unified Gauge-Based Analysis (CPCUGA; Chen et al. 2008). The CPCUGA data cover the conterminous United States (CONUS) at a 1/4° spatial resolution from 1948 to present (https://psl.noaa.gov/data/gridded/data.unified.daily.conus.html, accessed 4 March 2021).

Gauge distribution is geographically uneven and varies over time, presenting difficulties for applications that cover a wide domain or a period not sampled by a nearby station. Gridded meteorological datasets provide a useful alternative and are widely used in climate, agricultural, ecological, and hydrological applications. They provide uniform spatial and temporal coverage and generally apply quality control procedures to the underlying station data.

The choices made in station data processing can render a gridded dataset better suited for some applications than others. Most precipitation gauge data available in the CONUS are part of the National Weather Service Cooperative Observer Program (COOP; https://www.weather.gov/coop/overview, accessed 11 May 2020; McCarthy 2007) and are recorded once per day. The most common observation times are morning or early evening local time, with a trend away from evening observations in recent decades (Fig. 1; cf. Janis 2002). Hourly precipitation information is generally not available from such stations, although a few are first-order sites that have a weighing precipitation gauge. For the other stations, combining readings into a uniform time frame requires time adjustment methods based on the hour of observation, which may be unrecorded or incorrect (Belcher and Degaetano 2005). Time-adjustment methods can affect the statistics of precipitation extremes in the gridded product, as well as the wet day fraction (f_{wet}), wet spell length, and mean precipitation on wet days ($\overline{P}_{wet}$), rendering a time-adjusted product less suited to applications affected by such measures. On the other hand, time adjustment improves synchronicity between stations observed at different times and can provide a better match to

Supplemental information related to this paper is available at the Journals Online website: https://doi.org/10.1175/JHM-D-20-0212.s1.

Corresponding author: David W. Pierce, dpierce@ucsd.edu

DOI: 10.1175/JHM-D-20-0212.1

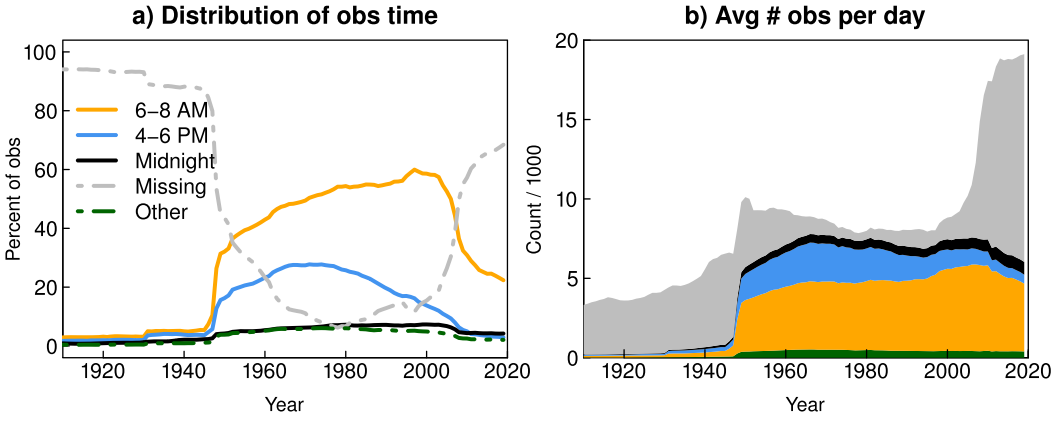

FIG. 1. (a) Distribution of precipitation gauge observation times (LST). (b) Average number of observations per day, calculated for each year. Observation time is indicated using the same colors as in (a).

calendar-day recording streamflow gauges when comparing a land surface model's simulated runoff to observations. Whether to use a gridded dataset that time adjusts station observations depends on the application but should be informed by what effects the processing method used has on the metrics of interest. The current work was motivated by the need for a gridded precipitation product for training a statistical downscaling scheme applied to global climate model projections. Accurately representing the statistics of extreme precipitation is paramount for such applications.

A related but separate issue to processing daily precipitation observations is how daily values can be disaggregated to hourly values for use in forcing a hydrological model. Assuming the daily total falls uniformly results in different runoff than using a more realistic approach (e.g., Bohn et al. 2019). Although this is an important consideration, in the current work we focus on daily values.

Livneh et al. (2013, hereafter L13) is a widely used gridded meteorological dataset that uses time adjustment when constructing the gridded daily precipitation fields. L13 has a 1/16° spatial resolution (~6 km) and covers the conterminous United States (plus the Columbia River basin in Canada) from 1915 to 2011. A later version using the same time adjustment and gridding methodology extended the domain to central Mexico through southern Canada, but at a shorter temporal coverage (1950–2013; Livneh et al. 2015, hereafter L15). L13 and L15 have their roots in an earlier gridded dataset with 1/8° (12 km) spatial resolution (Maurer et al. 2002), although with some methodological differences.

In this work we 1) examine how the time adjustment used in L13 and L15 alters f_{wet}, $\overline{P}_{\text{wet}}$, and extreme precipitation statistics and 2) introduce a new gridded precipitation dataset that is based on L13 but has no time adjustments, and so better represents f_{wet}, $\overline{P}_{\text{wet}}$, and extreme precipitation statistics in the gridded data. The new unadjusted precipitation data use the same 1/16° spatial resolution as L13 and L15 and are suited to applications that are sensitive to extreme precipitation statistics, such as flooding, and to ecological or land surface simulations that are affected by wet day fraction or mean precipitation on wet days. For example, wet day fraction affects the calculation of land surface forcing in the Mountain Climate Simulator (MT-CLIM) algorithm (Hungerford et al. 1989), which in turn affects runoff and evaporation in land surface models that incorporate such forcing (Gutmann et al. 2014; Vano et al. 2020). Historically, the Variable Infiltration Capacity land surface model (VIC; Liang et al. 1994) has often been driven this way. We also take the opportunity to extend the precipitation data through 2018, adding 7 more years to L13.

Examining precipitation statistics in L13 and L15 is important because they have been widely used in water resource and related applications. For example, Gutmann et al. (2014) examined L13 in the context of water resource assessments, including f_{wet} and daily extremes; Prein et al. (2016) examined precipitation trends in L13, including daily frequency and intensity; Li et al. (2017) trained a downscaling method on daily L13 to examine how precipitation and melting snow jointly determine runoff; Mahoney et al. (2016) and Gershunov et al. (2017) used L13 to assess daily heavy precipitation events due to landfalling atmospheric rivers in the southeastern and western United States, respectively; Gergel et al. (2017) used L13 precipitation and temperature to force a land surface model to examine wildfire potential; Chen et al. (2015) used L13 as the precipitation observations to evaluate model biases and bias correction methodologies, including in extreme daily precipitation; Lundquist et al. (2015) evaluated daily L13 precipitation against snow pillow observations in large winter storm events in the Sierra Nevada; Shields et al. (2018) nominated L13 as one of the observed daily precipitation datasets to use in evaluating different atmospheric river tracking methods; Lute et al. (2015) used L13 precipitation and temperature to train a statistical downscaling technique and examine projected changes in snowfall extremes and variability; Behnke et al. (2016) evaluated the suitability of L13 and other gridded precipitation and temperature datasets for ecological applications in the CONUS, including precipitation extremes and wet day counts; Ahmadalipour et al. (2017) used L13 as precipitation observations to evaluate global climate models in the Columbia River basin, including the variability of daily precipitation; Livneh and Hoerling (2016) used L15 to drive VIC

and examine drought processes in central North America; Walton et al. (2015) used L13 to evaluate a hybrid dynamic/statistical downscaling method in Southern California; Huang et al. (2017) used L13 as the historical basis for examining projected precipitation changes over the northeastern United States, including in extreme precipitation; and Pierce et al. (2014) used L15 precipitation and temperature to train a statistical downscaling method applied to 32 global climate models from the CMIP5 archive to produce the Localized Constructed Analogs (LOCA) dataset, which subsequently informed the Fourth California Climate Assessment (e.g., Pierce et al. 2018) and the Fourth National Climate Assessment (e.g., Hayhoe et al. 2017). The breadth and geographical diversity of applications using L13 and L15 precipitation motivates carefully examining the statistical properties of the gridded data.

The data and methods used to construct the unadjusted dataset will be outlined in section 2, but only briefly since they largely follow L13. Section 3 shows why the L13 time adjustment affects f_{wet}, $\overline{P}_{\text{wet}}$, and precipitation extremes, and how the unadjusted dataset introduced here compares to L13 in those measures. Not all applications are affected by the time adjustment, and others are more suited to the time-adjusted data. In section 4 we discuss limitations of both the unadjusted dataset introduced here and L13/L15, and how to choose between them for different applications. Conclusions are given in section 5.

2. Data and methods

The gridding method used here is identical to that used in L13 and L15, which in turn closely follow Maurer et al. (2002), and so will be only briefly summarized here. The exception is the time adjustment, which is discussed in detail in the following sections.

Once-daily precipitation data from the National Climatic Data Center (NCDC) COOP stations form the backbone of data used to construct the new dataset. Approximately 20 000 stations were used, and up to 12 000 at a single time. Only stations with at least 20 years of data were included.

The station data were spatially gridded using the SYMAP algorithm (Shepard 1984), a form of inverse distance weighting, following Maurer et al. (2002). The effects of topography at unobserved locations were accounted for by scaling to the PRISM (Daly et al. 1997, 2008) gridded climatology in the CONUS and Vose et al. (2014) in Canada, such that the monthly climatology of the SYMAP-interpolated station data was set to match the PRISM/Vose monthly climatological values. In brief, the ratio of monthly PRISM or Vose climatological precipitation to the same quantity in the interpolated dataset was computed for each month at every location over the climatological period of 1981–2010. This ratio was then applied to the daily gridded values at that location for the applicable month for all years. Details are given in L15.

Most germane to this work is how L13 and L15 time-adjust a time series of once-daily precipitation gauge values to a calendar day. Let $P^h(t)$ be a gauge observation on day t at hour h (in the range 0–23). Time adjustment to midnight ($h = 23$) is accomplished by

$$P^{23}(t) = P^h(t)\Delta + P^h(t+1)(1-\Delta), \quad (1)$$

where $\Delta = (h + 1)/24$. Figure 1 shows that that the most common gauge observation times are between 0600 and 0800 local standard time (LST). Time adjustment recognizes that for a gauge read in the morning, today's precipitation is largely reported in tomorrow's reading. Minutes are ignored in the adjustment, and $(h + 1)$ is used to calculate Δ so that observation times are rounded up to the next integer hour. For example, a 0530 LST observation time ($h = 5$) is rounded up to the next whole hour so that $\Delta = (h + 1)/24 = 6/24$. Missing observation times are not uncommon and increase in recent decades. In L13 missing observation times were set to midnight.

The new unadjusted version of the dataset introduced here omits the time adjustment in the processing. Any station report with a nominal 24-h ending time falling within the given calendar day (LST) is used (subject to quality checks and station data length requirements outlined in L13 and L15). As shown in section 3c, this reduces the errors in the gridded data's depiction of f_{wet}, $\overline{P}_{\text{wet}}$, and precipitation extremes. We also extended the time coverage of the data through 2018. The 1/16° spatial resolution of L13 and L15 is unchanged.

Hourly station observations

To understand how time adjustment affects the data, we use hourly precipitation values from the NOAA National Centers for Environmental Information (NCEI) Hourly Precipitation Data (HPD) Network, version 2 (https://www.ncei.noaa.gov/data/coop-hourly-precipitation/v2/access, accessed 11 May 2020) to form synthetic sequences of precipitation as would have been observed in a once-daily gauge read at 0700 LST, as well as the time series of true calendar day values. At each station, the calendar year was included in the analysis if at least 95% of the hourly observations were not missing. A minimum of four valid calendar years was required to include the station in the analysis, yielding 1913 stations. Different stations have different a different number of years included, with the median being 22 years, and 182 stations having at least 40 years included. Although some stations start in 1948, coverage improves in the early 1950s. The last year included was 2018.

3. Results comparing adjusted and unadjusted data

A simple schematic shows how time adjustment alters precipitation statistics (Fig. 2). In the 0530 LST gauge series (Fig. 2a), the maximum value over the illustrated period is 50.8 mm on 22 June 2010. Following Eq. (1) with $h = 5, \Delta = 1/4$ so each observation is split into two pieces, 1/4 of the total (pink blocks) and 3/4 of the total (blue blocks). The observed value is split this way because the observation time is rounded up to the next integer hour. The previous day's observation was 24 h ago, and 6 of those 24 h (1/4) occurred during the current calendar day, and 18 of those hours (3/4) occurred during the previous calendar day. Blocks are labeled by their original observed day number. Since the maximum value is observed on 22 June, the largest pink and blue blocks must also be on 22 June (indicated by the red stars).

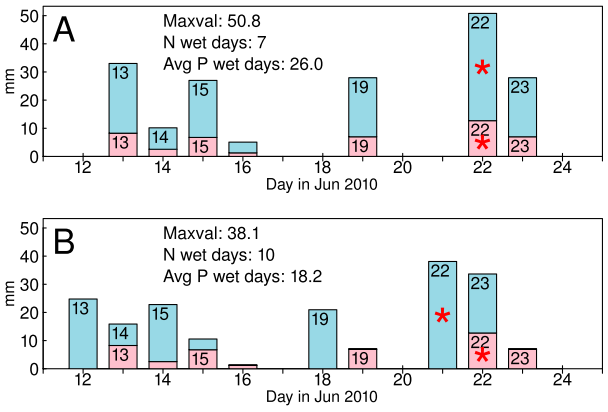

FIG. 2. Example time sequence of precipitation (a) after accumulating to a 0530 LST gauge observation time. Black numbers in the boxes refer to the day of the month. The pink blocks are 1/4 of the total gauge value, while the blue blocks are 3/4 of the total value. Red stars indicate the largest pink and blue blocks in the time series. (b) After time adjustment, the blue blocks are shifted one day earlier, while the pink blocks remain fixed.

To produce the time-adjusted data, each blue block is shifted earlier one day and added to the existing pink block (Fig. 2b). The maximum value is reduced, because the largest blue block (indicated by the star) is now added to a less-than-maximum pink block. Likewise, the largest pink block (starred) is added to a less-than-maximum blue block. Individual days can have a larger value after adjustment (days 12, 14, 18, and 21 in this example) but none of these can equal or exceed the original maximum since they are the sum of a blue and pink block where one or both are not the largest. Numerically, the maximum drops from 50.8 to 38.1 mm in this example. The number of wet days increases because the red blocks are fixed, so those days are wet in both Figs. 2a and 2b, but the shifted blue blocks create a new wet day whenever they are shifted into a previously dry day (days 12, 18, and 21). In this example, 7 wet days are transformed to 10 wet days. Total precipitation is conserved but spread over more wet days, so the average precipitation on wet days drops from 26.0 to 18.2 mm.

Although Fig. 2 shows the basics of why time adjustment alters precipitation statistics, this concept has been met with some surprise. Two common arguments are 1) precipitation is not locked to the diurnal cycle in most of the CONUS, so it should not matter whether extremes are computed with respect to the original observation time or after adjustment to local calendar days, and 2) a daily precipitation total is as likely to be increased in value by the procedure as decreased and therefore the changes average out, so time adjustment should have little effect on extreme statistics given enough samples. These arguments will be addressed theoretically (section 3a), by an empirical analysis using hourly gauge observations to construct a synthetic once-daily observed time series (section 3b), and via a direct comparison between extreme statistics of L13, the original station data, and the new unadjusted dataset introduced here (section 3c).

a. How time adjustment alters precipitation statistics

Precipitation can have appreciable diurnal variability depending on the location and season (e.g., Dai et al. 1999). However, in this section we consider a simplified case where no such synchronization is present (this assumption will be removed in the following sections). Under this assumption f_{wet}, $\overline{P}_{\text{wet}}$, and extreme precipitation statistics do not depend on the 24-h window they are calculated in, and calendar day statistics ($h = 23$) will be the same as those based on any other hour: $\overline{P}^{23}_{\text{wet}} = \overline{P}^{h}_{\text{wet}}$ and $f^{23}_{\text{wet}} = f^{h}_{\text{wet}}$ for all hours h.

The key point in addressing argument 1 above is understanding that Eq. (1) is only an *approximation* to a sequence of observations on calendar day intervals. Approximations have deficiencies, and it is easy to see why this particular approximation alters f_{wet} and $\overline{P}_{\text{wet}}$ at a station where $h \neq 23$. Consider a sequence of N wet days observed at hour h, $P^h(1, \ldots, N) > 0$, preceded and followed by dry days: $P^h(0) = 0$ and $P^h(N + 1) = 0$. Applying Eq. (1) to calculate $P^{23}(0)$, we have $P^{23}(0) = P^h(0)\Delta + P^h(1)(1 - \Delta)$. Since $P^h(1) > 0$ by construction, we must have $P^{23}(0) > 0$ despite $P^h(0) = 0$. In other words, Eq. (1) prepends a new wet day in $P^{23}(t)$ to a sequence of N wet days in $P^h(t)$, changing it to a sequence of $N + 1$ wet days. This is analogous to how moving the blue blocks left in Fig. 2 creates a new wet day at the start of every string of wet days. Therefore, the time adjustment increases time-adjusted f^{23}_{wet}. above the value f^{h}_{wet}. This violates the initial contention that the two quantities are equal and therefore is an error in the representation of wet day fraction in the time-adjusted data. Additionally, since Eq. (1) preserves total precipitation over the period of record (excluding end effects, which are negligible for a long record) the same total precipitation is spread over more wet days, making $\overline{P}^{23}_{\text{wet}} < \overline{P}^{h}_{\text{wet}}$. This again violates the initial contention that they are the same.

The reason extreme values are diminished by Eq. (1), and why argument 2 above (that effects compensate) is not valid even though individual nonmaximum days can be increased (Fig. 2), is as follows. Let the period extreme precipitation value $P^h(t_{\max})$ be higher than any other gauge value observed at hour h over some period, say a year (for yearly maximum precipitation). Since by construction $P^h(t_{\max})$ is larger than any other $P^h(t)$ value in the period, the gauge reading the day before the maximum can be written $P^h(t_{\max} - 1) = f_{-1}P^h(t_{\max})$ where $f_{-1} < 1$. That is, the gauge value read the day before the maximum gauge value must be a fraction (less than 1) of the maximum gauge value. Likewise for the day after the maximum gauge reading: $P^h(t_{\max} + 1) = f_{+1}P^h(t_{\max})$ where $f_{+1} < 1$. Then, $P^{23}(t_{\max} - 1)$, the time-adjusted precipitation reported for the previous calendar day, and $P^{23}(t_{\max})$, the time-adjusted value for the current calendar day, are by Eq. (1) (and dropping the "max" subscript):

$$P^{23}(t - 1) = P^h(t - 1)\Delta + P^h(t)(1 - \Delta), \tag{2}$$

$$P^{23}(t) = P^h(t)\Delta + P^h(t + 1)(1 - \Delta). \tag{3}$$

Using the f values defined above, we can rewrite these as

$$P^{23}(t - 1) = f_{-1}P^h(t)\Delta + P^h(t)(1 - \Delta) = P^h(t)(f_{-1}\Delta + 1 - \Delta), \tag{4}$$

$$P^{23}(t) = P^h(t)\Delta + f_{+1}P^h(t)(1-\Delta) = P^h(t)[\Delta + f_{+1}(1-\Delta)]. \quad (5)$$

If on day $t-1$ the time adjusted data were larger than the gauge observation, it would require $P^{23}(t-1) > P^h(t)$, so from the rightmost side of Eq. (4), $P^h(t)(f_{-1}\Delta + 1 - \Delta) > P^h(t)$, or $(f_{-1}\Delta + 1 - \Delta) > 1$ or $\Delta(f_{-1} - 1) > 0$, or (since Δ is positive) $f_{-1} > 1$ However, by construction $f_{-1} < 1$, and therefore it is impossible for the time adjusted value on the day preceding a gauge maximum to exceed the maximum gauge observation. In fact, the time adjusted value is always less than the maximum gauge value, unless two consecutive and identical maximum gauge observations are found—an unlikely occurrence since precipitation values tend to be strongly skewed with many small values and a few sparse high values.

If on day t the time adjusted data were larger than the original data, it would require $P^{23}(t) > P^h(t)$. Analogous algebra applied to the rightmost side of Eq. (5) leads to the requirement $f_{+1} > 1$, which is similarly impossible since $f_{+1} < 1$ by construction. Therefore, the time adjustment process of Eq. (1) produces smaller values than reported by the gauge on both the calendar day before and day of the maximum gauge observation.

What about $P^{23}(y)$ on days not immediately before or equal to the maximum day ($y \neq t_{\max}$ and $y \neq t_{\max} - 1$)? Those are easily shown to be less than $P^h(t_{\max})$ through a similar process as above, noting that since $P^h(t_{\max})$ is greater than every other value in the period by definition, all other values in the period can be expressed as some new factor $f' < 1$ times $P^h(t_{\max})$. For Eq. (1) to generate a new value $> P^h(t_{\max})$ would lead to similar requirements that the f values >1 despite them being <1. The one exception is at the ends of the period, where extreme days at the end of the previous period or beginning of the next period can produce a new in-period maximum after Eq. (1) is applied. The likelihood of this is low for long periods, however. In the limit that the distribution of precipitation is the same every day of the year (no seasonality) the chance this happens will scale as one over the period length. It is evaluated for actual stations, which do generally have seasonality, in the following section.

The increase in f_{wet} depends on the typical length wet day sequences and the hour of observation. For nonmidnight stations, the shorter the average sequence length, the more f_{wet} will be increased. In the limit that wet days always occur singly, time adjustment of a nonmidnight station would double f_{wet}. In the limit that wet days typically extend over an entire synoptic period, say 5 days, f_{wet} would be increased by a factor of 1.2. Most stations would fall between these two extremes.

The change in $\overline{P}_{\text{wet}}$ is the inverse of the change in f_{wet}, since total precipitation is conserved. Therefore, time-adjusted $\overline{P}_{\text{wet}}$ is 0.5 of the true calendar day value if wet days occur singly and 0.83 if wet days tend to occur 5 days in a row.

In summary, the time-adjustment method of Eq. (1) reduces the period-maximum precipitation value of nonmidnight stations, except in two rare circumstances: 1) an extreme occurs the day after the period ends and is shifted into the period or 2) if a gauge records two or more equal extreme values consecutively. The adjustment also increases the fraction of wet days and decreases the mean precipitation on wet days at stations that are not read at midnight. The key realization is that Eq. (1) is an *approximation* to a time series based on calendar days rather than the actual time series and has different statistical properties. Where precipitation is not locked to the diurnal cycle, extreme statistics could be calculated from gauges read at different hours and still be comparable. However, this is not true for calculations based on the time-adjusted data, since the approximation of Eq. (1) alters the extreme precipitation statistics.

b. *Evaluation using hourly precipitation observations*

An empirical approach to evaluating the effect of time adjustment on f_{wet}, $\overline{P}_{\text{wet}}$, and extreme precipitation statistics is to use hourly precipitation data (section 2) to construct a synthetic time series of once-daily precipitation gauge observations taken at some hour other than midnight, time-adjust the synthetic series into calendar days using Eq. (1), and compare the results to the hourly values aggregated to calendar days. The empirical approach complements the calculations in section 3a in that the seasonality and diurnal cycle of precipitation and different station observation hours are included, but differing periods of records, missing values, and data quality issues can affect the analysis.

Figure 3 shows the ratio of the average maximum daily precipitation in a year calculated from the time-adjusted synthetic 0700 LST time series to that calculated from the hourly data aggregated to calendar days and therefore experiencing no time adjustment. The values are averaged over all valid years (section 2) before the ratio is formed. On average, time adjustment for a 0700 LST station reduces the annual maximum precipitation value by a factor of 0.73 (Fig. 3a). Greater temporal coherence in extreme precipitation events gives less reduction due to the time-averaging process (factors closer to 1). The figure shows extreme precipitation along the West Coast is more temporally coherent than elsewhere in the CONUS. The least coherent extremes (smallest factors) are found in a band from Texas and Louisiana trough the Midwest. Different stations have the maximum reduced by a factor of 0.6–0.9 (Fig. 3b).

Figure 4 illustrates the effect of the time adjustment on wet day fraction in the synthetic 0700 LST observation hour time series, calculated across valid years in the same way as Fig. 3. On average, the time adjustment for a 0700 LST station increases wet day fraction by 53%, with the range across stations being 20%–75% (Fig. 4b).

c. *Comparing L13, the unadjusted data, and station observations*

We follow the analysis of Risser et al. (2019) in comparing extreme precipitation statistics between L13, the new unadjusted dataset, and Global Historical Climatology Network Daily (GHCN; Menne et al. 2012) once-daily precipitation observations over the CONUS. Precipitation extremes are illustrated as 20-yr return values obtained from a generalized extreme value (GEV) fit to the station observations, then gridding using a data-driven statistical approach (Risser et al. 2019).

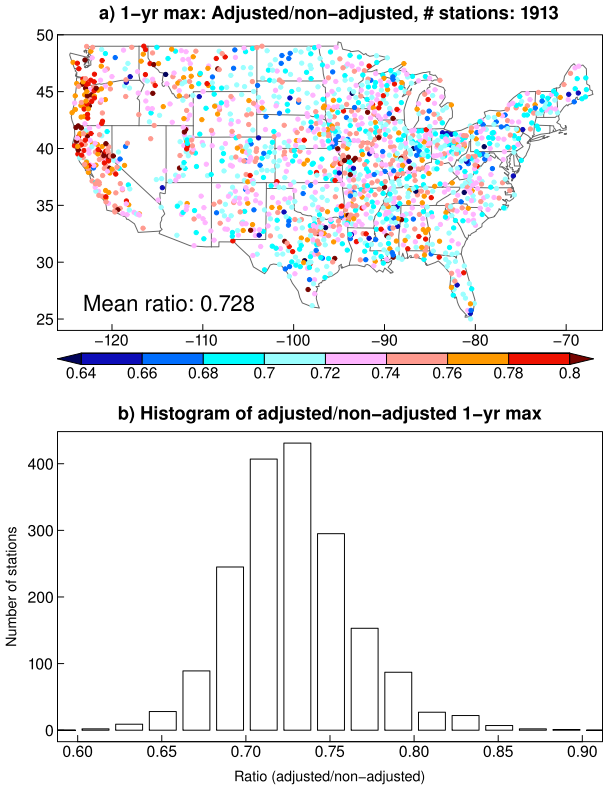

FIG. 3. (a) The ratio of average yearly maximum precipitation in the time-adjusted data divided by the value in the unadjusted (calendar day) data, at 1913 hourly stations. The time-adjusted data are computed on the basis of an idealized 0700 local standard observation time for all stations. (b) Histogram of the ratio values at the stations.

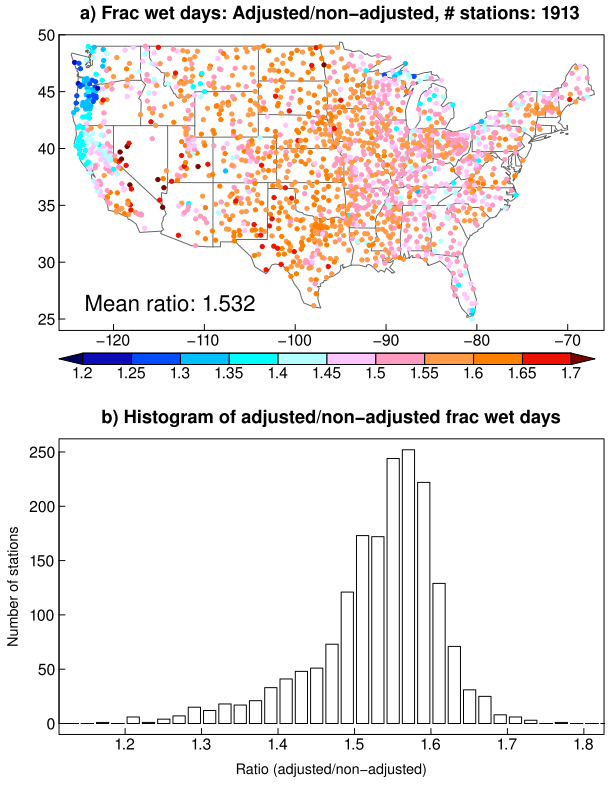

FIG. 4. (a) Alteration to wet-day fraction from the time adjustment, shown as the fraction of wet days in the time-adjusted data divided by wet day fraction in the nonadjusted (calendar day) data. The time-adjusted data are computed on the basis of an idealized 0700 local standard observation time for all stations. (b) Histogram of values across the stations.

Figure 5b shows the time-adjusted L13 data underestimate 20-yr return values over almost all the CONUS by about 30% (all seasons, and differences expressed as both mm day^{-1} and percent, are shown in Fig. S2 in the online supplemental material). The exception is parts of the Rocky Mountains and Sierra Nevada, likely due to Risser et al. (2019) using a simple linear adjustment with elevation (Risser et al. 2019, 2021, manuscript submitted to *Climatic Change*). L13 and L15 use a PRISM-based adjustment that includes other topographic considerations, such as vertical atmospheric layer, orographic effectiveness of the terrain, and slope orientation (Daly et al. 2008). Differences by season are evident as well, with more of an apparent overestimation of return values in winter (DJF) than summer (JJA). Since the methodology of Risser et al. (2019) does not depend on season, this suggests that some of the aspects influencing seasonal precipitation that are captured in the PRISM product reflect systematic summer–winter differences in precipitation mechanisms in the Rocky Mountains. The difficulty of estimating long-term precipitation from gauges in complex terrain due to insufficient high-elevation sampling and changing observation networks may also play a role (Henn et al. 2018). For example, of the approximately 5200 weather stations used in the Risser et al. (2019) product, 95% are below 1800-m elevation and 99% are below 2400 m.

The unadjusted data (Fig. 5c) show less underestimation of extreme precipitation values over most of the CONUS, with the bias dropping from ~30% to 4%–12%. A reduction in return values is still evident in the unadjusted data, with the largest reduction in summer and smallest in winter. Gutmann et al. (2014) also identified the low bias in extreme precipitation in L13 and attributed it to the gridding process. Averaging different extremes across a grid reduces the extrema, especially when the extrema are not spatially coherent, as one would expect to be more prevalent in summer. Gervais et al. (2014) illustrated this with gridding experiments, showing how extrema are reduced when calculated from gridded data versus when the station extreme statistics themselves are gridded. The analysis here shows the key role of the time-adjustment process in reducing extremes, but the reduction from gridding noted by Gervais et al. (2014), Gutmann et al. (2014), and Risser et al. (2021, manuscript submitted to *Climatic Change*) operates as well.

The fraction of wet days f_{wet} for L13 (top), the new unadjusted dataset (middle), and the ratio (L13/unadjusted) is shown in Fig. 6. Days are counted as wet if gridded precipitation exceeds 0.25 mm, chosen to be consistent with the 0.01 inch

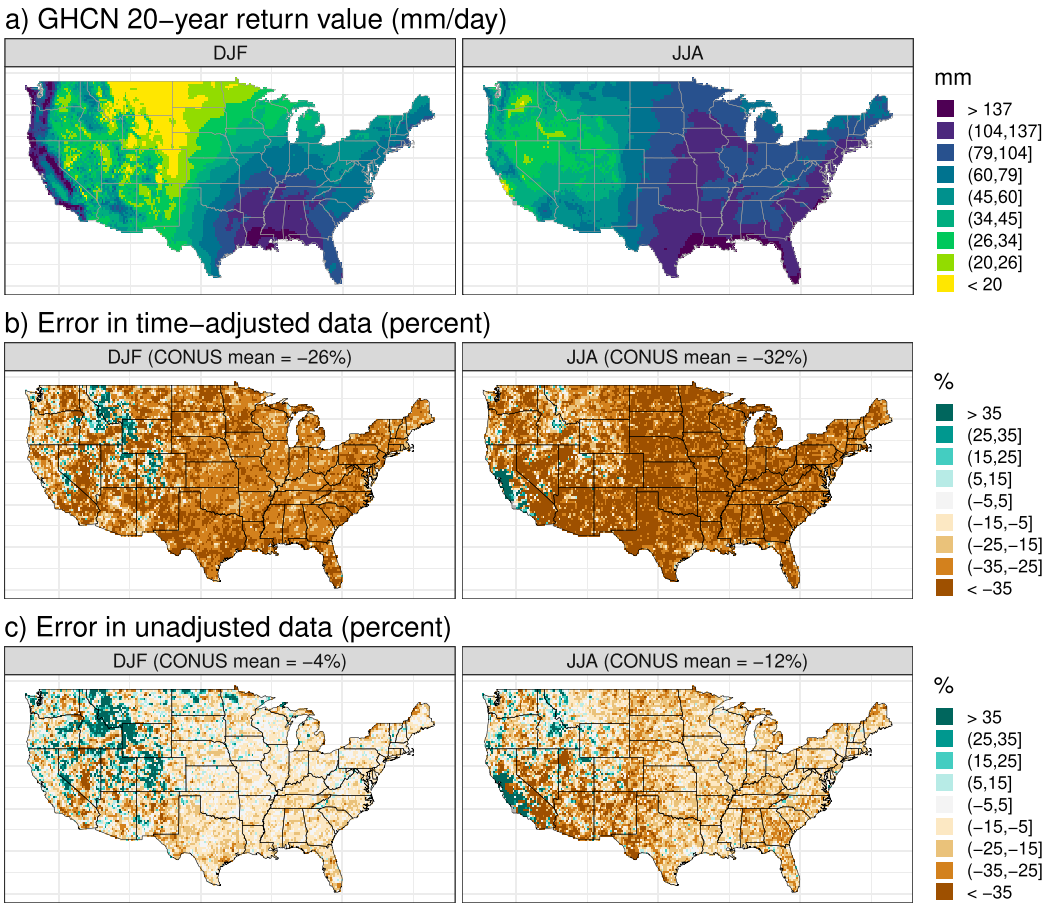

FIG. 5. (a) 20-yr return value of daily precipitation from the GHCN stations in (left) winter (December–February) and (right) summer (June–August). (b) Error with respect to the GHCN data in the gridded L13 time-adjusted data in winter and summer. (c) Error with respect to the GCHN data in the unadjusted gridded data in winter and summer.

reporting minimum for the Coop station data. The fraction of wet days f_{wet} is about 25% larger in the time-adjusted data compared to the unadjusted. Similar to Fig. 4, the largest increase in f_{wet} is seen in the dry regions of Nevada through the California deserts, and the smallest increase in the wet regions west of the Cascade Mountains in the Pacific Northwest. As noted in section 3, this is in accord with the expectation that increases will be largest in the driest regions and smallest in the wettest. The f_{wet} found in long GHCN-Daily stations is shown in Fig. S1. Even the unadjusted data have a higher f_{wet} than seen in the station data (31.7% versus 25.1% averaged over the CONUS), another outcome of the gridding process discussed above. Users who want to make f_{wet} match station observations could apply a threshold of ~0.8 mm to the new unadjusted data, which yields f_{wet} similar to the station data. Doing so would require increasing the nonzero amounts slightly to maintain the long-term average value. The change in $\overline{P}_{wet}$ is inversely proportional to the change in f_{wet}, and so is about a factor of 0.8 lower in the time-adjusted data than the unadjusted data.

As noted above, f_{wet} increases because the time adjustment adds a new wet day before a string of wet days at gauges that are not observed at midnight. Figure 7 shows wet spell length distributions for the unadjusted (blue) and time-adjusted (red) data averaged over four regions in the CONUS. The increase in mean wet spell length (indicated by the blue and red numbers on each panel) exceeds one day because wet spells that are separated by only one day in the original station data are combined into a single, longer wet spell after time adjustment. This is more likely to happen in wetter regions, so the relatively wet Pacific Northwest wet spell length is increased the most (2.5 days), while the relatively dry southwestern United States increased the least (1.5 days). In the unadjusted data the most common wet spell length is 1 day, except in the southeastern United States where it is 2 days. After time adjustment, this is increased by a day. There are still 1-day wet spells after time adjustment because some stations observe at midnight, notably many of the long-record, high-quality airport stations.

4. Discussion

a. *Effect of precipitation time adjustment on hydrology*

To explore how the changes in f_{wet}, $\overline{P}_{wet}$, and extreme precipitation statistics might affect hydrology, we ran the VIC land surface model (version 4.2.c) twice, once with the adjusted

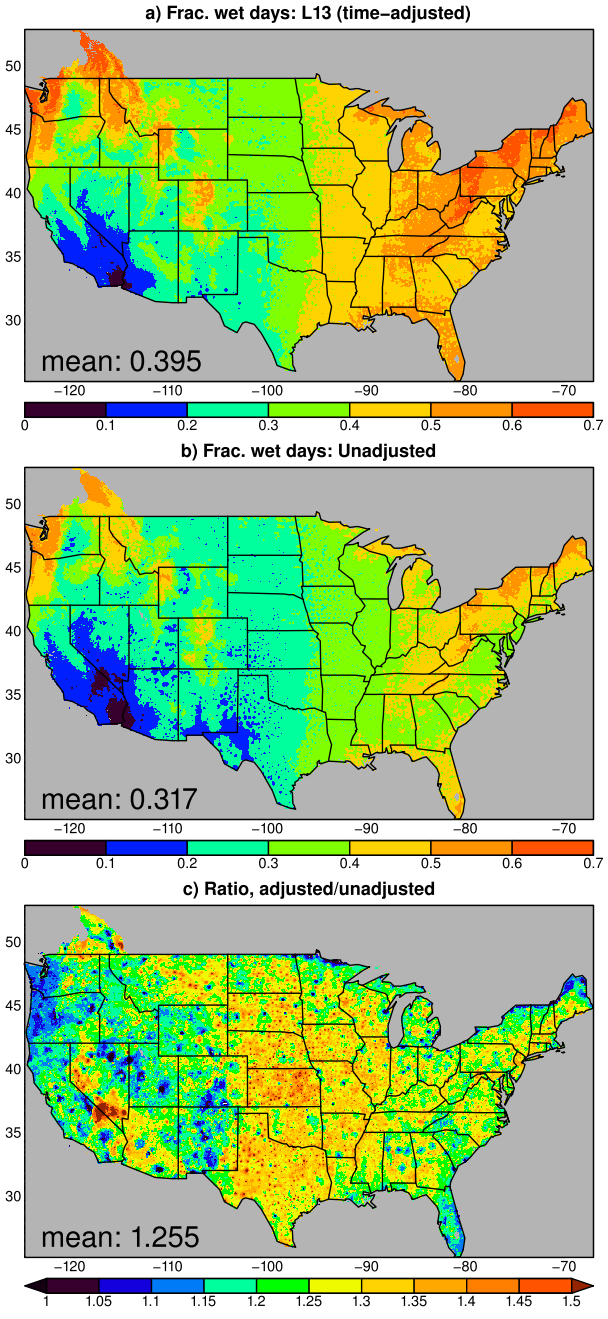

FIG. 6. (top) Fraction of wet days (precipitation > 0.25 mm) in the L13 (time-adjusted) data. (middle) The unadjusted data. (bottom) Ratio, fraction of wet days in the adjusted over unadjusted data.

(L13) precipitation and once with the new, nonadjusted precipitation dataset developed here. The VIC model calibration parameters were downloaded from https://ciresgroups.colorado.edu/livneh/data (accessed 17 August 2020). As listed in Hamman et al. (2018; their Table 1) VIC has been used for a wide range of applications, including constructing retrospective datasets of hydrological variables over both the CONUS and world (Maurer et al. 2002; Sheffield et al. 2006), evaluation of historical trends in snow, streamflow, and drought (Mote et al. 2005; Tan et al. 2011; Nijssen et al. 2014); climate change analysis (Barnett et al. 2005; Gergel et al. 2017), and coupled land–atmosphere modeling (Zhu et al. 2009, Hamman et al. 2016). A comprehensive evaluation of VIC, albeit of a previous version, is given in Xia et al. (2018). Additionally, VIC participated in the Water Model Intercomparison Project (WaterMIP), with a summary of how VIC simulates global water balance compared to several other land surface and global hydrological models available in Haddeland et al. (2011). Xia et al. (2012) show that VIC simulates streamflow reasonably well compared to observations across much of the CONUS.

We compared VIC output from the two runs over the period 1950–2011, with the start determined by when the majority of stations begin reporting observation time (Fig. 1). VIC was run with a daily input time step without imposing any subdaily precipitation time distribution. Temperatures were from L13 and held constant between the two runs. Differences between several fields (unadjusted with respect to time-adjusted) are shown in Fig. 8. For reference, annual maximum 1-day precipitation increases 27% in the final unadjusted dataset (Fig. 8a), not surprising given how time adjustment reduces extreme precipitation statistics (Figs. 3 and 5). Similarly, VIC annual maximum 1-day snowfall increases 29% (not shown). Annual maximum 1-day total runoff (surface plus baseflow) increases 38% averaged over the domain (Fig. 8b), more than the increase in maximum 1-day precipitation due to the nonlinear nature of runoff. In much of the central United States from Texas through North Dakota, annual 1-day maximum runoff increases more than 50%, which would affect flood simulations in those regions.

Although it is not surprising that annual maximum 1-day runoff increases given that annual maximum 1-day precipitation increases, VIC shows more subtle runoff responses as well. The unadjusted precipitation has more pronounced peaks and higher $\overline{P}_{\text{wet}}$. Both increase runoff efficiency compared to the time-adjusted data, which are smoother in time and so yield a lower runoff efficiency. As a result, annual mean total runoff is 17% higher when VIC is driven by the unadjusted data (Fig. 8c), and 20%–40% higher over a wide swatch of the central United States. Seasonally, domain averaged increases in runoff increase the most in summer (20%) and least in winter (14%; not shown).

Total precipitation is conserved by the time adjustment [Eq. (1)] except for small discrepancies ($\sim$0.6%) due to missing value handling in the adjustment process. In either one of the two VIC runs the water balance averaged over the full run is runoff = precipitation–evapotranspiration (ET), neglecting changes in soil moisture, which are small over the individual multidecade runs. (Note that soil moisture can be different between the two VIC runs, however.) The increase in runoff and fixed precipitation therefore mandates a decrease in ET, which drops 2.3% averaged over the domain in the unadjusted run (Fig. 8d). ET shows a smaller percentage drop than runoff even though the changes in mm day^{-1} are equal but oppositely signed because ET exceeds runoff by a considerable margin

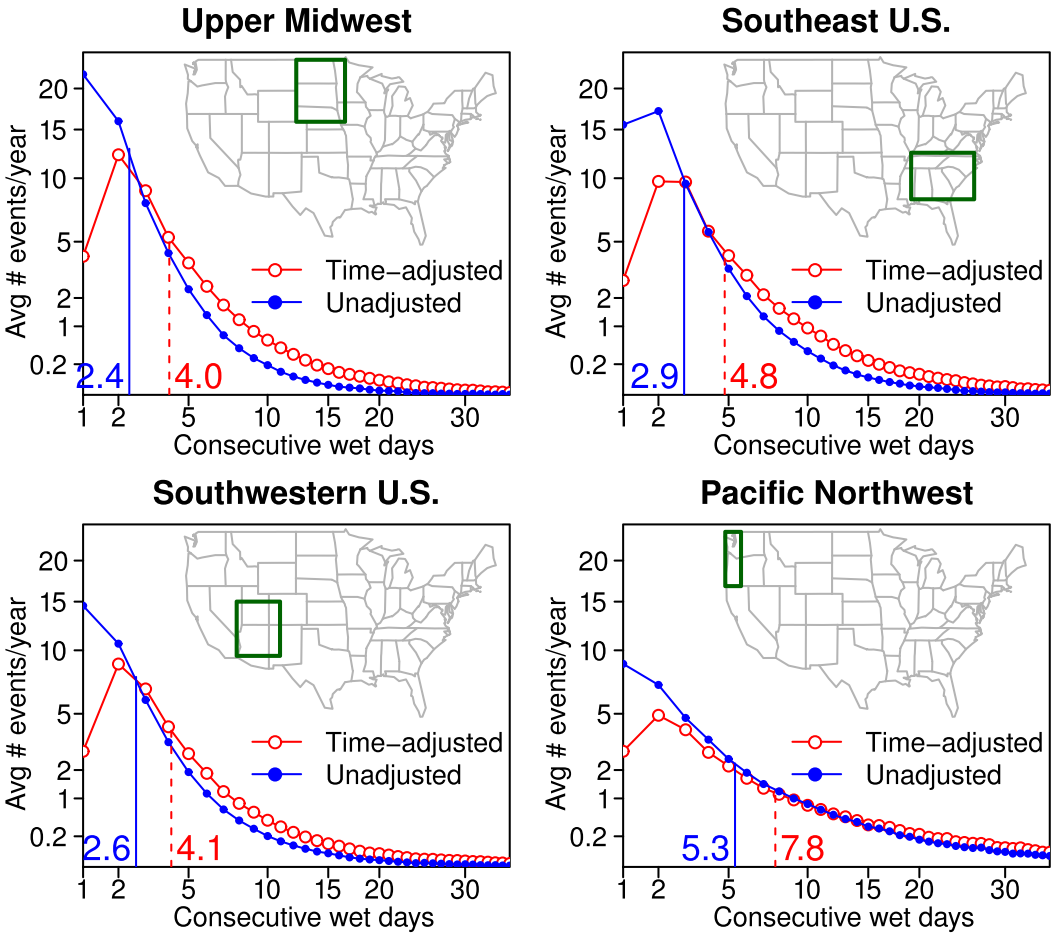

FIG. 7. Distribution of wet spell length (days), shown as the average number of spells of the indicated length per year, averaged over four regions in the CONUS. Blue shows the unadjusted data, and red shows the data after time adjustment. Vertical lines and numbers show the mean wet spell length. The green box in the inset map shows the region being averaged over.

over much of the United States, rendering a constant value change a smaller percentage change. ET decreases exceed 6% over parts of the U.S. Southeast. With reduced ET the latent heat flux drops by 2.2% as well, again with the largest decreases over the Southeast (Fig. 8e).

Versions of VIC before version 5 incorporate the MT-CLIM algorithms (Hungerford et al. 1989). As noted in Gutmann et al. (2014) and Vano et al. (2020), MT-CLIM uses the presence or absence of precipitation to influence cloudiness and therefore surface downwelling solar insolation, which increases 3.3% in the unadjusted run due to the lower fraction of wet days (Fig. 8f). Annual maximum 1-day snowmelt increases as well, by 10% over snowy regions (defined as averaging at least 0.5 cm SWE in winter; not shown).

b. *Dataset selection*

Combining precipitation observations from gauges with differing observation times into a uniform time frame is not straightforward and involves tradeoffs. L13 time-adjusted the observations to a uniform calendar day, while the new unadjusted dataset described here omits the time adjustments. What applications are better suited to the split versus unadjusted data, and what applications are not affected?

First, applications that use monthly averaged precipitation are not affected by the time adjustment process (e.g., Mazdiyasni and AghaKouchak 2015). Second, applications that are dependent on daily-scale synchronicity across different stations likely can make use of the time adjustment process, which puts stations observed at different times on a uniform basis. Even then it should be noted that many stations do not include an observation time (Fig. 1) and are set to midnight in L13 and L15, which degrades the synchronicity since it is unlikely that all the missing stations actually observe at midnight.

On the other hand, the more an application is affected by daily statistics, the less appropriate it is to use the time-adjusted dataset. The adjustment process decreases annual maximum 1-day precipitation by 27%, and annual maximum 1-day VIC runoff by 38%. Even mean annual runoff decreases appreciably in the time-adjusted data (17%), which could be of concern in large-scale water balance studies. Likewise, wet-spell

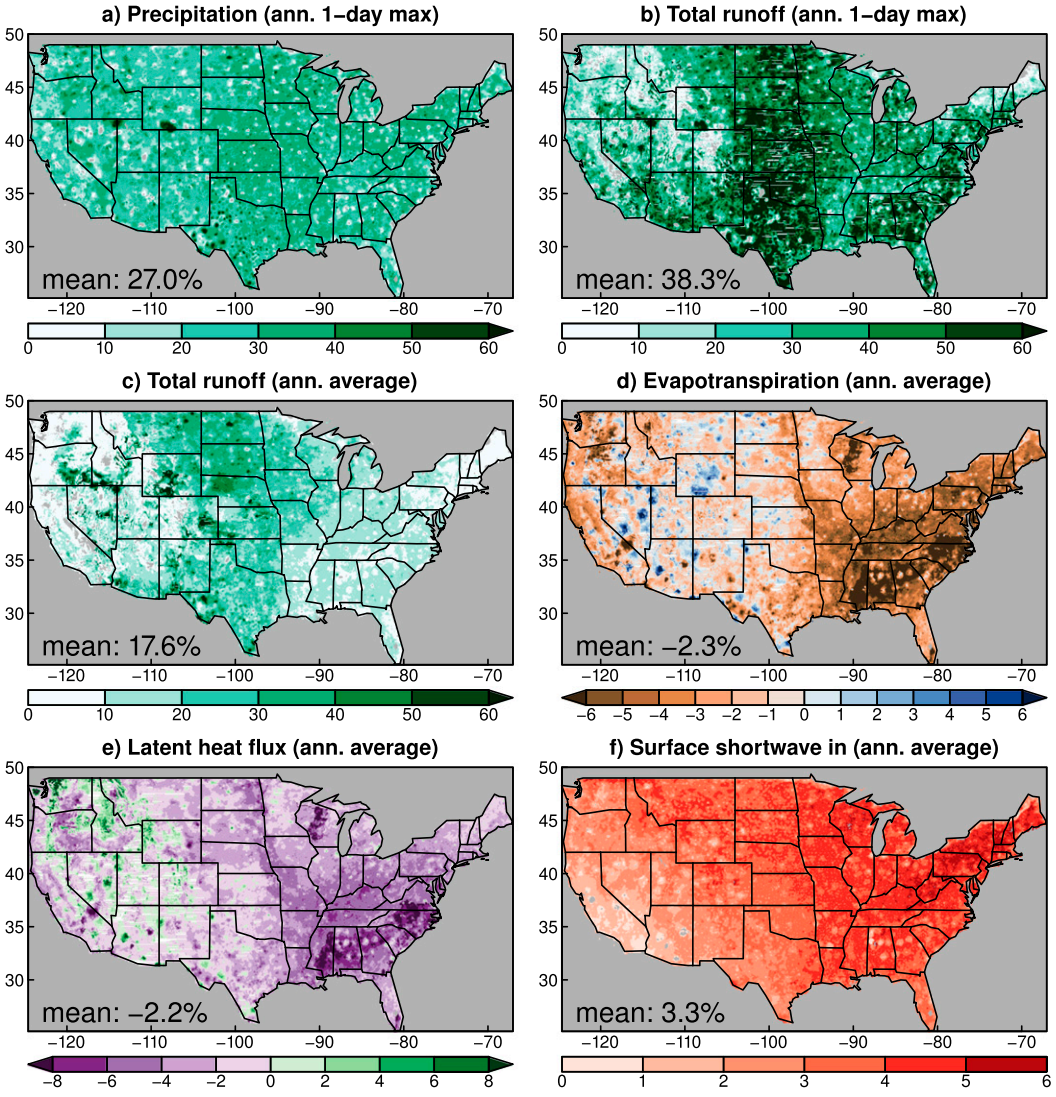

FIG. 8. Change (percent) when the VIC land surface model is forced with the new unadjusted precipitation data, compared to being forced with L13 (time-adjusted) precipitation. Some panels are annual average 1-day maximum values while others are annual averages, as indicated in the titles.

statistics are skewed by the time-adjustment process. Although the fraction of wet days is affected substantially and the MT-CLIM algorithm uses this as a predictor of surface forcing, the resultant change in surface incoming solar radiation is modest (3.3%), and so may make only a limited difference to ecological simulations.

c. *Models as the way forward?*

Recent discussions have suggested that model-based precipitation datasets may become increasingly attractive as model quality improves, obviating problems with the gauge records, including irregular and biased spatial coverage, inconsistent and incomplete temporal sampling, and changing station composition (e.g., Jing et al. 2017; Lundquist et al. 2019). A model-based precipitation dataset avoids problems with time adjustment noted here, and so is attractive from that point of view. However, many applications need the long time series gauge-based records offer, which considerably exceed the time span of the satellite era (ca. 1979 onward). One way forward could be to combine the model and gauge based precipitation records to produce a merged dataset with the strengths of both. This approach was used by Abatzoglou (2013), but in that work was limited to the satellite era. As high-quality model based reanalyses are progressively pushed further back in time, this approach could provide ever longer hybrid meteorological datasets.

5. Conclusions

Constructing a daily gridded precipitation dataset from observations taken at different times of the day has surprisingly strong implications for regional hydroclimate and extreme

precipitation and runoff events. Generating such a dataset involves compromises since the underlying gauge observations are taken under a variety of conditions. In this work we have examined the implications of differing times of observation and the outcome of two different data processing choices, either time adjusting the once-daily gauge readings (as done in L13 and L15) or avoiding this step. Our results will help researchers better assess whether to use the time-adjusted or unadjusted data developed here by providing a better understanding of each selection's implications.

One of our main findings is that a daily time adjustment that partitions observed precipitation across two days, such as used in L13 and L15, has significant consequences. This adjustment mutes extreme precipitation values, with annually averaged 1-day maximum precipitation in the time-adjusted data 27% lower than in the unadjusted data, and the 20-yr return value of daily precipitation 30% lower. Comparing these metrics to the underlying station data shows that the unadjusted data are far closer to the observed daily station values than the time-adjusted data.

Similarly, the time-adjusted data show 25% more wet days than the unadjusted data, and again, the unadjusted data are a better match to the original station data. The gridding process reduces the precipitation extremes and increases the fraction of wet days, so even the unadjusted data underestimate 20-yr daily precipitation return values by ~10%, underestimate the annual mean 1-day maximum precipitation by about 10%, and portray an unrealistically large fraction of wet days (0.32 versus 0.26, averaged over the domain). Nevertheless, these errors in the unadjusted data are significantly smaller than those found in the time-adjusted data.

The unadjusted gridded precipitation dataset developed here extends L13 by 7 years and has the same 1/16° spatial resolution as L13 and L15. It will be used for training a statistical downscaling scheme, where correctly capturing daily extremes and other statistics of precipitation is of primary importance. Other applications, such as studies involving monthly total or average precipitation, may be little affected by whether the time-adjusted or unadjusted data are used. Yet other applications that examine daily runoff in a limited region and compare to streamflow gauges might prefer the time-adjusted data. However, even then it should be kept in mind that the time adjustment process has a notable effect on both daily and annual runoff (as portrayed by the VIC hydrological model). The results presented here will assist in selecting the proper gridded daily precipitation dataset for the intended application.

Acknowledgments. This project was funded by contract RC19-1391 from the Strategic Environmental Research and Development Program (SERDP) and NOAA's RISA California–Nevada Climate Applications Program Award NA17OAR4310284. Additional support was provided by California Energy Commission contract EPC-16-063, DOE Award DE-SC0014333, the California Department of Water Resources Award 4600013361, and the U.S. Department of the Interior via the Southwest Climate Adaptation Science Center (G18AC00320). This work was improved by comments from anonymous reviewers, which are gratefully acknowledged.

Data availability statement. The gridded precipitation data with no time adjustment can be downloaded from ftp://livnehpublicstorage.colorado.edu/public/sulu/Prec_unsplit_CONUS_Canada_1915_2018/.

REFERENCES

Abatzoglou, J. T., 2013: Development of gridded surface meteorological data for ecological applications and modelling. *Int. J. Climatol.*, **33**, 121–131, https://doi.org/10.1002/joc.3413.

Ahmadalipour, A., A. Rana, H. Moradkhani, and A. Sharma, 2017: Multi-criteria evaluation of CMIP5 GCMs for climate change impact analysis. *Theor. Appl. Climatol.*, **128**, 71–87, https://doi.org/10.1007/s00704-015-1695-4.

Barnett, T. P., J. C. Adam, and D. P. Lettenmaier, 2005: Potential impacts of a warming climate on water availability in snow-dominated regions. *Nature*, **438**, 303–309, https://doi.org/10.1038/nature04141.

Behnke, R., S. Vavrus, A. Allstadt, T. Albright, W. E. Thogmartin, and V. C. Radeloff, 2016: Evaluation of downscaled, gridded climate data for the conterminous United States. *Ecol. Appl.*, **26**, 1338–1351, https://doi.org/10.1002/15-1061.

Belcher, B. N., and A. T. Degaetano, 2005: A method to infer time of observation at US Cooperative Observer Network stations using model analyses. *Int. J. Climatol.*, **25**, 1237–1251, https://doi.org/10.1002/joc.1183.

Bohn, T. J., K. M. Whitney, G. Mascaro, and E. R. Vivoni, 2019: A deterministic approach for approximating the diurnal cycle of precipitation for use in large-scale hydrological modeling. *J. Hydrometeor.*, **20**, 297–317, https://doi.org/10.1175/JHM-D-18-0203.1.

Chen, M., P. Xie, and CPC Precipitation Working Group, 2008: CPC Unified gauge-based analysis of global daily precipitation. *2008 Western Pacific Geophysics Meeting*, Cairns, Queensland, Australia, Amer. Geophys. Union, 14 pp., https://ftp.cpc.ncep.noaa.gov/precip.orig/CPC_UNI_PRCP/GAUGE_GLB/DOCU/Chen_et_al_2008_Daily_Gauge_Anal.pdf.

Chen, J., F. P. Brissette, and P. Lucas-Picher, 2015: Assessing the limits of bias-correcting climate model outputs for climate change impact studies. *J. Geophys. Res. Atmos.*, **120**, 1123–1136, https://doi.org/10.1002/2014JD022635.

Dai, A., F. Giorgi, and K. E. Trenberth, 1999: Observed and model-simulated diurnal cycles of precipitation over the contiguous United States. *J. Geophys. Res.*, **104**, 6377–6402, https://doi.org/10.1029/98JD02720.

Daly, C., G. H. Taylor, and W. P. Gibson, 1997: The PRISM approach to mapping precipitation and temperature. Preprints, *10th Conf. on Applied Climatology*, Reno, NV, Amer. Meteor. Soc., 20–23.

——, M. Halbleib, J. I. Smith, W. P. Gibson, M. K. Doggett, G. H. Taylor, J. Curtis, and P. P. Pasteris, 2008: Physiographically sensitive mapping of climatological temperature and precipitation across the conterminous United States. *Int. J. Climatol.*, **28**, 2031–2064, https://doi.org/10.1002/joc.1688.

Donat, M. G., A. L. Lowry, L. V. Alexander, P. A. O'Gorman, and N. Maher, 2016: More extreme precipitation in the world's dry and wet regions. *Nat. Climate Change*, **6**, 508–513, https://doi.org/10.1038/nclimate2941.

Gergel, D. R., B. Nijssen, J. T. Abatzoglou, D. P. Lettenmaier, and M. R. Stumbaugh, 2017: Effects of climate change on snowpack and fire potential in the western USA. *Climatic Change*, **141**, 287–299, https://doi.org/10.1007/s10584-017-1899-y.

Gershunov, A., T. Shulgina, F. M. Ralph, D. A. Lavers, and J. J. Rutz, 2017: Assessing the climate-scale variability of atmospheric rivers affecting western North America. *Geophys. Res. Lett.*, **44**, 7900–7908, https://doi.org/10.1002/2017GL074175.

Gervais, M., L. B. Tremblay, J. R. Gyakum, and E. Atallah, 2014: Representing extremes in a daily gridded precipitation analysis over the United States: Impacts of station density, resolution, and gridding methods. *J. Climate*, **27**, 5201–5218, https://doi.org/10.1175/JCLI-D-13-00319.1.

Groisman, P. Ya., and D. R. Legates, 1994: The accuracy of United States precipitation data. *Bull. Amer. Meteor. Soc.*, **75**, 215–227, https://doi.org/10.1175/1520-0477(1994)075<0215:TAOUSP>2.0.CO;2.

Gutmann, E., T. Pruitt, M. P. Clark, L. Brekke, J. R. Arnold, D. A. Raff, and R. M. Rasmussen, 2014: An intercomparison of statistical downscaling methods used for water resource assessments in the United States. *Water Resour. Res.*, **50**, 7167–7186, https://doi.org/10.1002/2014WR015559.

Haddeland, I., and Coauthors, 2011: Multimodel estimate of the global terrestrial water balance: Setup and first results. *J. Hydrometeor.*, **12**, 869–884, https://doi.org/10.1175/2011JHM1324.1.

Hamman, J. J., and Coauthors, 2016: The land surface climate in the regional Arctic system model. *J. Climate*, **29**, 6543–6562, https://doi.org/10.1175/JCLI-D-15-0415.1.

——, B. Nijssen, T. J. Bohn, D. R. Gergel, and Y. Mao, 2018: The Variable Infiltration Capacity model version 5 (VIC-5): Infrastructure improvements for new applications and reproducibility. *Geosci. Model Dev.*, **11**, 3481–3496, https://doi.org/10.5194/gmd-11-3481-2018.

Hayhoe, K., J. Edmonds, R. E. Kopp, A. N. LeGrande, B. M. Sanderson, M. F. Wehner, and D. J. Wuebbles, 2017: Climate models, scenarios, and projections. Climate Science Special Report: Fourth National Climate Assessment, Vol. I, D. J. Wuebbles Eds., U.S. Global Change Research Program, 133–160, https://doi.org/10.7930/J0WH2N54.

Henn, B., A. J. Newman, B. Livneh, C. Daly, and J. D. Lundquist, 2018: An assessment of differences in gridded precipitation datasets in complex terrain. *J. Hydrol.*, **556**, 1205–1219, https://doi.org/10.1016/j.jhydrol.2017.03.008.

Huang, H., J. M. Winter, E. C. Osterberg, R. M. Horton, and B. Beckage, 2017: Total and extreme precipitation changes over the northeastern United States. *J. Hydrometeor.*, **18**, 1783–1798, https://doi.org/10.1175/JHM-D-16-0195.1.

Hungerford, R. D., R. R. Nemani, S. W. Running, and J. C. Coughlan, 1989: MTCLIM: A mountain microclimate simulation model. USDA Forest Service Intermountain Research Station Research Paper INT-414, 56 pp., https://www.fs.fed.us/rm/pubs_int/int_rp414.pdf.

Janis, M. J., 2002: Observation-time-dependent biases and departures for daily minimum and maximum air temperature. *J. Appl. Meteor.*, **41**, 588–603, https://doi.org/10.1175/1520-0450(2002)041<0588:OTDBAD>2.0.CO;2.

Jing, X., B. Geerts, Y. Wang, and C. Liu, 2017: Evaluating seasonal orographic precipitation in the interior western United States using gauge data, gridded precipitation estimates, and a regional climate simulation. *J. Hydrometeor.*, **18**, 2541–2558, https://doi.org/10.1175/JHM-D-17-0056.1.

Knapp, A. K., C. Beier, D. D. Briske, A. T. Classen, Y. Luo, M. Reichstein, and J. L. Heisler, 2008: Consequences of more extreme precipitation regimes for terrestrial ecosystems. *BioScience*, **58**, 811–821, https://doi.org/10.1641/B580908.

Li, D., M. L. Wrzesien, M. Durand, J. Adam, and D. P. Lettenmaier, 2017: How much runoff originates as snow in the western United States, and how will that change in the future? *Geophys. Res. Lett.*, **44**, 6163–6172, https://doi.org/10.1002/2017GL073551.

Liang, X., D. P. Lettenmaier, E. F. Wood, and S. J. Burges, 1994: A simple hydrologically based model of land surface water and energy fluxes for general circulation models. *J. Geophys. Res.*, **99**, 14 415–14 428, https://doi.org/10.1029/94JD00483.

Livneh, B., and M. P. Hoerling, 2016: The physics of drought in the U.S. Central Great Plains. *J. Climate*, **29**, 6783–6804, https://doi.org/10.1175/JCLI-D-15-0697.1.

——, E. A. Rosenberg, C. Lin, B. Nijssen, V. Mishra, K. M. Andreadis, E. P. Maurer, and D. P. Lettenmaier, 2013: A long-term hydrologically based dataset of land surface fluxes and states for the conterminous United States: Update and extensions. *J. Climate*, **26**, 9384–9392, https://doi.org/10.1175/JCLI-D-12-00508.1.

——, T. Bohn, D. W. Pierce, F. Munoz-Arriola, B. Nijssen, R. Vose, D. R. Cayan, and L. Brekke, 2015: A spatially comprehensive, hydrometeorological data set for Mexico, the U.S., and southern Canada 1950–2013. *Sci. Data*, **2**, 150042, https://doi.org/10.1038/sdata.2015.42.

Lundquist, J. D., M. Hughes, B. Henn, E. D. Gutmann, B. Livneh, J. Dozier, and P. Neiman, 2015: High-elevation precipitation patterns: Using snow measurements to assess daily gridded datasets across the Sierra Nevada, California. *J. Hydrometeor.*, **16**, 1773–1792, https://doi.org/10.1175/JHM-D-15-0019.1.

——, ——, E. Gutmann, and S. Kapnick, 2019: Our skill in modeling mountain rain and snow is bypassing the skill of our observational networks. *Bull. Amer. Meteor. Soc.*, **100**, 2473–2490, https://doi.org/10.1175/BAMS-D-19-0001.1.

Lute, A. C., J. T. Abatzoglou, and K. C. Hegewisch, 2015: Projected changes in snowfall extremes and interannual variability of snowfall in the western United States. *Water Resour. Res.*, **51**, 960–972, https://doi.org/10.1002/2014WR016267.

Mahoney, K., and Coauthors, 2016: Understanding the role of atmospheric rivers in heavy precipitation in the southeast United States. *Mon. Wea. Rev.*, **144**, 1617–1632, https://doi.org/10.1175/MWR-D-15-0279.1.

Maurer, E. P., A. W. Wood, J. C. Adam, D. P. Lettenmaier, and B. Nijssen, 2002: A long-term hydrologically based dataset of land surface fluxes and states for the conterminous United States. *J. Climate*, **15**, 3237–3251, https://doi.org/10.1175/1520-0442(2002)015<3237:ALTHBD>2.0.CO;2.

Mazdiyasni, O., and A. AghaKouchak, 2015: Substantial increase in concurrent droughts and heatwaves in the United States. *Proc. Natl. Acad. Sci. USA*, **112**, 11 484–11 489, https://doi.org/10.1073/pnas.1422945112.

McCarthy, D., 2007: Cooperative station observations. National Weather Service Manual Rep. 10-1315, 122 pp.

Menne, M. J., I. Durre, R. S. Vose, B. E. Gleason, and T. G. Houston, 2012: An overview of the global historical climatology network-daily database. *J. Atmos. Oceanic Technol.*, **29**, 897–910, https://doi.org/10.1175/JTECH-D-11-00103.1.

Mote, P. W., A. F. Hamlet, M. P. Clark, and D. P. Lettenmaier, 2005: Declining mountain snowpack in western North America. *Bull. Amer. Meteor. Soc.*, **86**, 39–50, https://doi.org/10.1175/BAMS-86-1-39.

Nijssen, B., S. Shukla, C. Lin, H. Gao, T. Zhou, J. Sheffield, E. F. Wood, and D. P. Lettenmaier, 2014: A prototype global drought information system based on multiple land surface models. *J. Hydrometeor.*, **15**, 1661–1676, https://doi.org/10.1175/JHM-D-13-090.1.

Pierce, D. W., D. R. Cayan, and B. L. Thrasher, 2014: Statistical downscaling using localized constructed analogs (LOCA). *J. Hydrometeor.*, **15**, 2558–2585, https://doi.org/10.1175/JHM-D-14-0082.1.

——, J. F. Kalansky, and D. R. Cayan, 2018: Climate, drought, and sea level rise scenarios for California's Fourth Climate Change Assessment. Rep. CCCA4-CEC-2018-006, California Energy Commission, 78 pp., https://www.energy.ca.gov/sites/default/files/2019-11/Projections_CCCA4-CEC-2018-006_ADA.pdf.

Prein, A. F., G. J. Holland, R. M. Rasmussen, M. P. Clark, and M. R. Tye, 2016: Running dry: The U.S. Southwest's drift into a drier climate state. *Geophys. Res. Lett.*, **43**, 1272–1279, https://doi.org/10.1002/2015GL066727.

Risser, M. D., C. J. Paciorek, M. F. Wehner, T. A. O'Brien, and W. D. Collins, 2019: A probabilistic gridded product for daily precipitation extremes over the United States. *Climate Dyn.*, **53**, 2517–2538, https://doi.org/10.1007/s00382-019-04636-0.

Sheffield, J., G. Goteti, and E. F. Wood, 2006: Development of a 50-year high-resolution global dataset of meteorological forcings for land surface modeling. *J. Climate*, **19**, 3088–3111, https://doi.org/10.1175/JCLI3790.1.

Shepard, D. S., 1984: Computer mapping: The SYMAP interpolation algorithm. *Spatial Statistics and Models*, G. L. Gaile and C. J. Willmott, Eds., D. Reidel, 133–145.

Shields, C. A., and Coauthors, 2018: Atmospheric River Tracking Method Intercomparison Project (ARTMIP): Project goals and experimental design. *Geosci. Model Dev.*, **11**, 2455–2474, https://doi.org/10.5194/gmd-11-2455-2018.

Smith, A. B., 2020: U.S. billion-dollar weather and climate disasters, 1980 - present (NCEI Accession 0209268). NOAA National Centers for Environmental Information, accessed 27 May 2020, https://doi.org/10.25921/stkw-7w73.

Tan, A., J. C. Adam, and D. P. Lettenmaier, 2011: Change in spring snowmelt timing in Eurasian Arctic rivers. *J. Geophys. Res.*, **116**, D03101, https://doi.org/10.1029/2010JD014337.

Vano, J., and Coauthors, 2020: Comparing downscaled LOCA and BCSD CMIP5 climate and hydrology projections. U. S. Bureau of Reclamation, 90 pp., http://gdo-dcp.ucllnl.org/downscaled_cmip_projections/techmemo/LOCA_BCSD_hydrology_tech_memo.pdf.

Vose, R. S., and Coauthors, 2014: Improved historical temperature and precipitation time series for U.S. climate divisions. *J. Appl. Meteor. Climatol.*, **53**, 1232–1251, https://doi.org/10.1175/JAMC-D-13-0248.1.

Walton, D. B., F. Sun, A. Hall, and S. Capps, 2015: A hybrid dynamical-statistical downscaling technique. Part I: Development and validation of the technique. *J. Climate*, **28**, 4597–4617, https://doi.org/10.1175/JCLI-D-14-00196.1.

Xia, Y., and Coauthors, 2012: Continental-scale water and energy flux analysis and validation for North American Land Data Assimilation System project phase 2 (NLDAS-2): 2. Validation of model-simulated streamflow. *J. Geophys. Res.*, **117**, D03110, https://doi.org/10.1029/2011JD016051.

——, and Coauthors, 2018: Comprehensive evaluation of the Variable Infiltration Capacity (VIC) model in the North American land data assimilation system. *J. Hydrometeor.*, **19**, 1853–1879, https://doi.org/10.1175/JHM-D-18-0139.1.

Zhu, C., R. L. Leung, D. Gochis, Y. Qian, and D. P. Lettenmaier, 2009: Evaluating the influence of antecedent soil moisture on variability of the North American Monsoon precipitation in the coupled MM5/VIC modeling system. *J. Adv. Model. Earth Syst.*, **1**, 22, https://doi.org/10.3894/james.2009.1.13.